

HOMFLY-PT Polynomials of Open Links

Kenneth C. Millett
Department of Mathematics
University of California, Santa Barbara, CA, USA
Eleni Panagiotou*
University of Tennessee at Chattanooga
Chattanooga, TN, USA

February 16, 2022

Dedicated to the memory of Sir Vaughan Frederick Randal Jones.

Abstract

We numerically estimate the superposition of the HOMFLY-PT polynomial of an open two component link, define its spread, and describe how this quantity may be employed to quantify the degree of entanglement of confined two component open links.

1 Introduction

Many physical materials are composed of filamentous structures, such as macromolecules, and are mathematically modeled as collections of open simple curves in space. The entanglement of these molecules, reflected in the entanglement of the modeled curves, has a significant influence on the mechanical properties and function of such materials [4, 3, 26]. However, it has been a challenge to rigorously define a mathematical measure of entanglement in such systems. Panagiotou, [22, 21, 19] has employed the Gauss linking integral to create measures of entanglement in periodic boundary condition models of such systems. For the case of a single curve, i.e. an open knot, Millett et al. [14, 15], used the HOMFLY-PT [6] knot polynomial to define the probability distribution of knot types on the ensemble of closures of the endpoints of the curve over the 2-sphere of directions in space giving spectrum of the open knot and its dominate knot types. The superposition of this spectrum defines the average of the HOMFLY-PT polynomials of the ensemble of closures. Panagiotou and Kauffman [9] provide a rigorous definition of the Jones [8] polynomial of open chains via averaging the Jones polynomial of projections of an open curve (thereby

*EP was supported by NSF DMS 1913180

defining a knotoid) over all possible projection directions. The Jones polynomial of open curves is a polynomial with real coefficients that are continuous functions of the chain coordinates. As the endpoints of the chain tend to coincidence they converge to those of the Jones polynomial of the resulting closed curve. Note that the definition of the HOMFLY-PT polynomial of open arc diagrams (knotoids) is not yet defined. As a consequence, we employ an extension of the MDS method [14] for knots to the case of open links. Thus, whereas the superposition of the HOMFLY-PT S^2 pdf of MDS gave the average closure HOMFLY-PT polynomial of the knot, the superposition of the HOMFLY-PT $S^2 \times S^2$ pdf of closures of the two component open link gives the average closure HOMFLY-PT polynomial of the link.

We compare our results to those provided by an application of the Gauss linking number employed in the study of entanglement of polymer gels, [19].

Our estimation of the average HOMFLY-PT is achieved by determining the HOMFLY-PT polynomial and, therefore, the associated oriented link type at each pair of points in an independent uniformly distributed collection of 49 closure directions on each of the two spheres thereby giving a collection of 2401 samples. One can understand this procedure as providing an estimation of the integration of the HOMFLY-PT on the $S^2 \times S^2$ space of pairs of closure directions divided by the four dimensional volume of $S^2 \times S^2$. One of the fundamental properties of this method is that the proportion of link types of pairs of open chains converges to that of the closed chains as the distance between the two termini of each chain, respectively, goes to zero. We will explore this convergence in the case of a Hopf link.

As was observed in the study of protein structures, the linking spectrum depends on the specific geometry of the chain [15, 27, 25]. To examine the effect of the local geometry, we will consider the influence of the location of the gap in a closed chain as well as the effect of the spatial geometry of the chain. We will also study HOMFLY-PT polynomial of random pair of disjoint random walks, i.e. a random pair of disjoint equilateral polygons, in the 3-ball as their length increases.

This paper is organized as follows: In Section 2, by way of introduction to the study of complex two component open links, we study the link spectrum of an open Hopf link and its dependence on the location of the endpoints of the open link. In Section 3, we describe the foundation of our analysis starting with the definition of the average closure HOMFLY-PT polynomial of an open two component links in 3-space. In Section 4, we present results on the HOMFLY-PT polynomial of confined open two component links.

2 The HOMFLY-PT polynomial of open Hopf links

The HOMFLY-PT polynomial of a closed negative Hopf link, Figure 1, is



Figure 1: For a closed negative Hopf link, the HOMFLY-PT polynomial is: $(\ell + \ell^3) m^{-1} - \ell m$.

$$(\ell + \ell^3) m^{-1} - \ell m$$

The polynomial of the mirror reflection, the closed positive Hopf link, is given by replacing ℓ by ℓ^{-1} giving

$$(\ell^{-3} + \ell^{-1}) m^{-1} - \ell^{-1} m$$

To illustrate the properties of the average HOMFLY-PT polynomial, we apply our method to the case of open Hopf links for a small collection of gap openings in the closed link. The collection of 2401 closures can contain links of different topological types, see Figure 2. For a fixed gap size, the character of the entanglement, as reflected in the average HOMFLY-PT of open Hopf links can vary, depending on the location of the gap, see Figure 3 and Table 1. In these instances one observes that the dominate terms are those of the Hopf link and the secondary terms reflect the varying position of the gap.

2.1 Convergence as gap length goes to zero

As the gap, the segment connecting the termini, lengths of an open two component link go to zero we know the link type converges to the closed link type, i.e. the proportion of closures having the link type as the closed link goes to 1. What is the nature of this convergence, for example, how is this reflected in the evolution of the average HOMFLY-PT polynomial? Suppose one considers




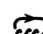





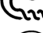
	P	F
0_1^2	 $(-\ell^{-1}-\ell)m^{-1}$	$(a^{-1}+a)x^{-1}-1$
2_1^2	 $(\ell+\ell^3)m^{-1}-\ell m$	$(-a-a^3)x^{-1}+a^2+(a+a^3)x$
4_1^2	 $(-\ell^3-\ell^5)m^{-1}+(3\ell^3+\ell^5)m-\ell^3m^3$	$(a^3+a^5)x^{-1}-a^4+(-3a^3-2a^5+a^7)x+(a^4+a^6)x^2+(a^3+a^5)x^3$
4_1^2	 $(-\ell^{-5}-\ell^{-3})m^{-1}+(\ell^{-3}-\ell^{-1})m$	$(a^{-5}+a^{-3})x^{-1}-a^{-4}+(-3a^{-5}-2a^{-3}+a^{-1})x+(a^{-4}+a^{-2})x^2+(a^{-5}+a^{-3})x^3$
5_1^2	 $(-\ell^{-1}-\ell)m^{-1}+(\ell^{-1}+2\ell+\ell^3)m-\ell m^3$	$(a^{-1}+a)x^{-1}-1+(-2a^{-1}-4a-2a^3)x+(-1+a^4)x^2+(a^{-1}+3a+2a^3)x^3+(1+a^2)x^4$
6_1^2	 $(\ell^5+\ell^7)m^{-1}+(-6\ell^5-3\ell^7)m+(5\ell^5+\ell^7)m^3$ $-\ell^5m^5$	$(-a^5-a^7)x^{-1}+a^6+(6a^5+4a^7-a^9+a^{11})x+(-3a^6-2a^8+a^{10})x^2+(-5a^5-4a^7+a^9)x^3$ $+(a^6+a^8)x^4+(a^5+a^7)x^5$
6_1^2	 $(\ell^{-7}+\ell^{-5})m^{-1}+(-\ell^{-5}+\ell^{-3}-\ell^{-1})m$	$(-a^{-7}-a^{-5})x^{-1}+a^{-6}+(6a^{-7}+4a^{-5}-a^{-3}+a^{-1})x+(-3a^{-6}-2a^{-4}+a^{-2})x^2$ $+(-5a^{-7}-4a^{-5}+a^{-3})x^3+(a^{-6}+a^{-4})x^4+(a^{-7}+a^{-5})x^5$
6_2^2	 $(\ell^{-7}+\ell^{-5})m^{-1}+(-\ell^{-7}-2\ell^{-5}+2\ell^{-3})m$ $+(\ell^{-5}-\ell^{-3})m^3$	$(-a^{-7}-a^{-5})x^{-1}+a^{-6}+(-2a^{-9}+3a^{-7}+3a^{-5}-2a^{-3})x+(-a^{-6}-2a^{-4}-a^{-2})x^2$ $+(a^{-9}-2a^{-7}-2a^{-5}+a^{-3})x^3+(a^{-8}+2a^{-6}+a^{-4})x^4+(a^{-7}+a^{-5})x^5$
6_2^2	 $(-\ell^3-\ell^5)m^{-1}+(2\ell^3-\ell^5-\ell^7)m$ $+(-\ell^3+\ell^5)m^3$	$(a^3+a^5)x^{-1}-a^4+(-2a^3-a^5-a^7)x+(-3a^6-3a^8)x^2+(a^3+a^5)x^3$ $+(a^4+3a^6+2a^8)x^4+(a^5+a^7)x^5$
6_3^2	 $(-\ell^{-5}-\ell^{-3})m^{-1}+(2\ell^{-3}+\ell^{-1}+\ell)m-\ell^{-1}m^3$	$(a^{-5}+a^{-3})x^{-1}-a^{-4}+(-2a^{-5}-a^{-3}-a)x+(-3a^{-2}-3)x^2+(a^{-5}+a)x^3$ $+(a^{-4}+3a^{-2}+2)x^4+(a^{-3}+a^{-1})x^5$

Figure 2: The HOMFLY-PT and Kauffman polynomials of the simplest closed links [13]

Open Hopf link	average HOMFLY-PT polynomial	Gauss linking
A	$(0.001666\ell^{-3} - 0.088432\ell^{-1} + 0.824656\ell + 0.909204\ell^3) m^{-1}$ $+ (0.001249\ell^{-1} - 0.905873\ell) m - 0.001666\ell^{-1} m^3$	0.930618
B	$(0.158251\ell^{-3} - 0.4679854\ell^{-1} - 0.406038\ell + 0.218636\ell^3) m^{-1}$ $+ (-0.156689\ell^{-1} - 0.218636\ell) m$	0.013390
C	$(0.079966\ell^{-3} - 0.392753\ell^{-1} - 0.0320699\ell + 0.439400\ell^3) m^{-1}$ $+ (-0.0787172\ell^{-1} - 0.439400\ell) m$	0.444706
D	$(0.027072\ell^{-3} - 0.252395\ell^{-1} + 0.403582\ell + 0.681799\ell^3) m^{-1}$ $+ (-0.258226\ell^{-1} - 0.681799\ell) m$	0.729073
E	$(0.001666\ell^{-3} - 0.09745939\ell^{-1} + 0.78842149\ell + 0.8875468\ell^3) m^{-1}$ $+ (-0.001666\ell^{-1} - 0.8875468\ell) m$	0.86317

Table 1: The average HOMFLY-PT polynomials and Gauss linking numbers for the open Hopf links shown in Figure 3.

a polygonal positive Hopf link, see Figures 3 and associated data tables. We show what happens to the proportion of 0_1^2 's, $\pm 2_1^2$'s, and 4_1^2 's as the gap length decreases in Figure 4. Curiously, the limiting $+2_1^2$ is less likely than -2_1^2 when this particular gap becomes large.

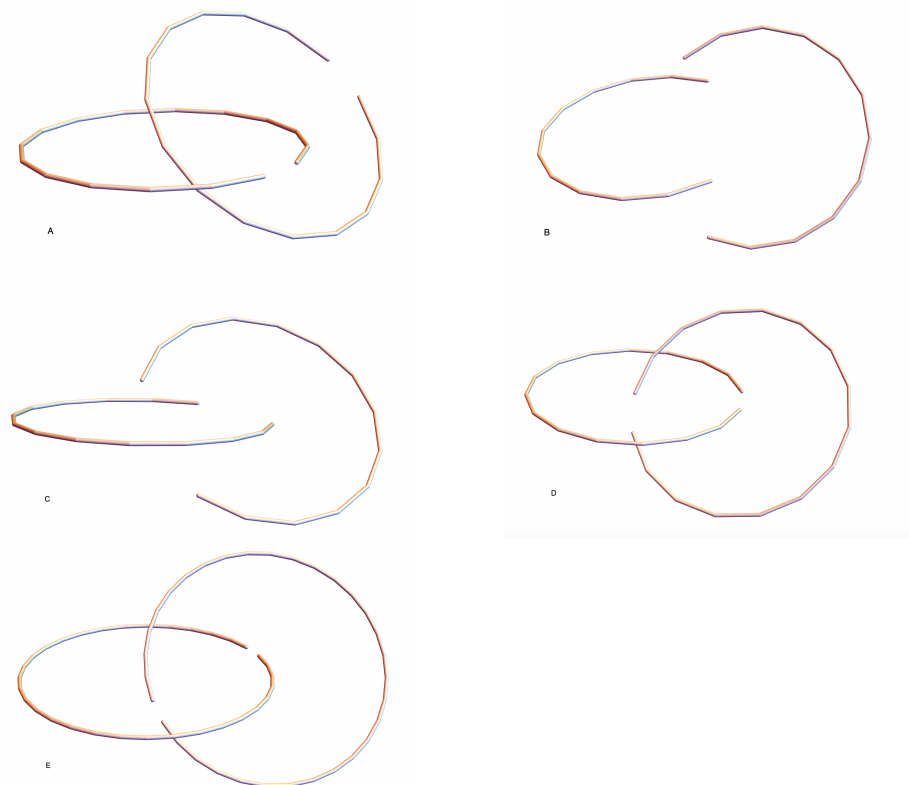


Figure 3: (A) A partial open negative Hopf link A: 49×49 closures give 0_1^2 , $\pm 2_1^2$, $\pm 4_1^2$, and 5_1^2 link types, Table 2 in the appendix. (B) The partial open positive Hopf link B: closures give 0_1^2 and $\pm 2_1^2$, link types. The gap is 1.66294, Table 3. (C) The partial open positive Hopf link C: closures give 0_1^2 , $\pm 2_1^2$, and 4_1^2 link types. The gap is 1.17286, Table 4. (D) The partial open positive Hopf link D: closures give 0_1^2 , $\pm 2_1^2$, and 4_1^2 link types. The gap is 0.390177, Table 5. (E) The partial open positive Hopf link E: closures give 0_1^2 , $\pm 2_1^2$, and 4_1^2 link types. The gap is 0.196034, Table 6.

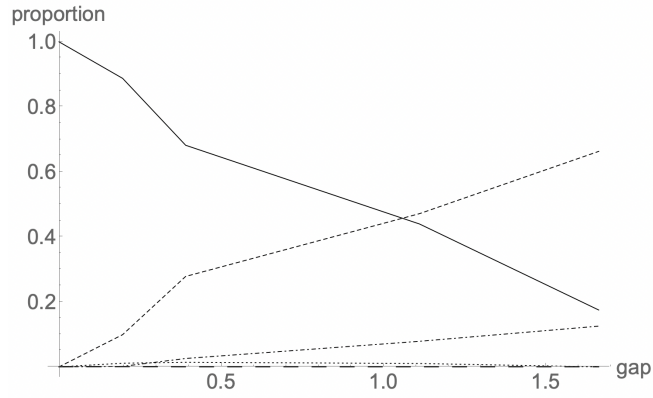


Figure 4: The proportion of link types for the closures as a function of the gap size: 0_1^2 ; dashed, 2_1^2 ; solid, -2_1^2 ; dash-dot, 4_1^2 ; dotted and 4_1^2 ; large dashed.

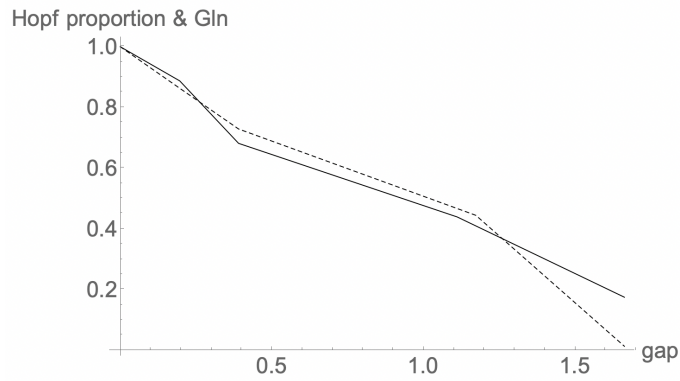


Figure 5: The proportion of positive Hopf links, solid, and the Gauss linking number, dashed, versus the gap.

3 Measures of Linking and Entanglement

In this section we will review the classical Gauss linking number, and we will explore how the average HOMFLY-PT polynomial can be used to quantify the entanglement present in two component links.

3.1 The Gauss linking number

The Gauss linking integral defines a *linking number* for a pair of disjoint oriented chains, closed or open, L_1 and L_2 , described by piecewise C^1 parameterizations, $\gamma_1(t)$ and $\gamma_2(s)$, $0 \leq t, s \leq 1$, is defined by the double integral:

$$Lk(L_1, L_2) = \frac{1}{4\pi} \int_{[0,1]} \int_{[0,1]} \frac{(\dot{\gamma}_1(t), \dot{\gamma}_2(s), \gamma_1(t) - \gamma_2(s))}{\|\gamma_1(t) - \gamma_2(s)\|^3} dt ds, \quad (1)$$

where $(\dot{\gamma}_1(t), \dot{\gamma}_2(s), \gamma_1(t) - \gamma_2(s))$ is the triple product of the derivatives, $\dot{\gamma}_1(t)$ and $\dot{\gamma}_2(s)$, and of the difference $\gamma_1(t) - \gamma_2(s)$.

While this is an integer for closed chains, it is a real number that captures the linking of a pair of oriented open chains finding application in many scientifically important context such as polymer melt models employing periodic boundary conditions; Panagiotou [22, 21, 19, 2]; complex systems such as Olympic gels [7]; protein structures [24, 23, 17, 18]. In Graph 5, we compare the proportion of positive Hopf links and the Gauss linking number.

For example, the Gauss linking number of the oriented open link shown in Figure 15 is 1.12954.

3.2 The average HOMFLY-PT polynomial as a measure of entanglement

We propose to define the average HOMFLY-PT of a pair of oriented open curves in 3-space as the superposition HOMFLY-PT polynomial over the pdf of $S^2 \times S^2$ independent closures for pairs of chains thereby providing a new quantification of the degree of entanglement present in the link. In the following we will examine the relationship between the Gauss linking integral and the average HOMFLY-PT polynomial.

3.2.1 The presence of the Gauss linking number in the HOMFLY-PT polynomial of a closed link

Suppose that $L = \{L_1, L_2, \dots, L_c\}$ is an oriented closed link of c components and λ is the total Gauss linking number of L , i.e. the sum of the $c(c-1)/2$ pairs of linking numbers between distinct components of L . Collecting the powers of m , we may express the HOMFLY-PT polynomial of L by

$$P_L(\ell, m) = \sum_{j=1-c} p_j(\ell) m^j$$

and of any component L_i by,

$$P_{L_i}(\ell, m) = \sum_{j=0} p_j^i(\ell) m^j$$

The following proposition is proved in [12]:

Proposition 3.1. *Proposition 22 [12] For an oriented link L , the powers of ℓ and m which appear in P_L are all even or all odd, depending upon whether the number of components of L , c , is odd or even, respectively. The exponent of the lowest power of m which appears is precisely $1 - c$. It has the coefficient*

$$p_{1-c}(\ell) = (-\ell^2)^{-\lambda} (-(\ell^{-1} + \ell))^{c-1} \prod_{i=1}^c p_0^i(\ell).$$

where λ is the total Gauss linking number of L , i.e. the sum of the $c(c-1)/2$ pairs of linking numbers between distinct components of L .

For example, for the negative Hopf link, Figure 1, one has

$$p_{-1}(\ell) = (-\ell^2)^1 (-(\ell^{-1} + \ell))^1 = \ell + \ell^3.$$

Due to the simplicity of the open Hopf links conformations analyzed here, one can detect the HOMFLY-PT polynomial of the closures by inspection of Table 1. One observes that the dominant terms in the average HOMFLY-PT polynomial over the 2401 closures correspond to these powers of ℓ and the proportion of closures that give the negative Hopf link. We observe that this relationship to the closed negative Hopf link is equally reflected in the coefficient of the ℓm term, again due to the simplicity of these links.

We have seen how to extend the Gauss linking number to collections of oriented open chains. Here, we consider if this proposition can be extended to oriented open links. Consider the oriented open two component polygonal link, $RL6 = \{L_1, L_2\}$ in Figure 15, where we can estimate P_{RL6} , P_{RL6_1} , and P_{RL6_2} .

In the case of open chains, the estimates of $p_{-1}(\ell)$, $p_0^1(\ell)$, and $p_0^2(\ell)$ are, individually, the superposition of a complex collection of terms each of which come from the closures of these open chains. While the term $(-(\ell^{-1} + \ell))$ is common to all and, therefore, would appear in the left side of the expression, the resulting total expression reflects the superposition of a collection of terms in which the linking number depends on the closures as do each of the polynomials of the individual components. As a consequence, due to the complexity of the links, one can only propose that the coefficient, $p_{1-c}(\ell)$, is average of the

equation 3.2.1 applied to the $S^2 \times S^2$ closures of the two component open oriented links. Consider the case of RL6, Figure 15.

$$p_{-1}(\ell) = (0.000416\ell^{-9} - 0.011291\ell^{-7} - 0.284465\ell^{-5} + 0.319034\ell^{-3} + 0.449396\ell^{-1} - 0.155352\ell - 0.005831\ell^3)$$

$$p_0^1(\ell) = (-0.000781\ell^{-4} - 0.014531\ell^{-2} + 0.964219 - 0.032656\ell^2 - 0.0090625\ell^4)$$

$$p_0^2(\ell) = (0.000313\ell^{-6} - 0.00875\ell^{-4} - 0.0185937\ell^{-2} + 0.989219 - 0.02046875\ell^2 - 0.00109375\ell^4)$$

$$(-\ell^2)^{-1}(-(\ell^{-1} + \ell))p_0^1(\ell)p_0^2(\ell) \approx (0.00044574\ell^{-9} - 0.00850606\ell^{-7} - 0.0409534\ell^{-5} + 0.922805\ell^{-3} + 0.902953\ell^{-1} - 0.0612069\ell - 0.00912977\ell^3 + 0.000231128\ell^5).$$

In the final product expression, the unknotted character of the two components is strongly reflected in the ℓ^{-3} and ℓ^{-1} coefficients whilst, it seems, this is lost in p_{-1} of the link, at least is so far as one might anticipate a relationship of the type expressed in the proposition manifested in coefficients. This divergence illustrates the strong entanglement complexity mixing the Gauss linking and the superposition of the HOMFLY-PT polynomials of the two component link closures.

3.2.2 The HOMFLY-PT polynomial

In the previous section we discussed the relationship between the m^{-1} term of a two component chain, the two m^0 terms of the two individual components, and the Gauss linking number of the two components, Prop 22 [12]. While we do not know of an analogous relationship reflected in the higher order components of the HOMFLY-PT polynomial examples show that they reflect the complexity of the entanglement of the two components, see Figure 2 and, for example, the Whitehead link 5_1^2 . Note that these classical link examples illustrate the conclusions of Prop 22, e.g. compare the initial terms of the trivial link and the Whitehead link. Furthermore, in reversing the orientation of the Solomon link 4_1^2 , one does not merely change ℓ to $\frac{1}{\ell}$ but there are higher order term consequences illustrating the HOMFLY-PT polynomial sensitivity to linking beyond the linking number, even for unknotted components or homologically unlinked cases such as the trivial link and the Whitehead link. As a consequence, one anticipates reflections of these complexities in the spectrum of closures of open two component links.

3.2.3 An open link example

As discussed earlier, we have found that, for open links, the relationship for classical closed links described in Prop 22 holds for open links in the sense that it is a convolution of Gauss linking terms and those coming from the HOMFLY-PT polynomials of the individual chains of the closure spectrum. Consider the average HOMFLY-PT polynomial for $RL6$, an open oriented two component case discussed earlier,

$$P_{RL6_1} = (-0.000781\ell^{-4} - 0.014531\ell^{-2} + 0.964219 - 0.032656\ell^2 - 0.0090625\ell^4) + (0.0007813\ell^{-2} + 0.0129687 + 0.0090625\ell^2)m^2$$

$$P_{RL6_2} = (0.000313\ell^{-6} - 0.00875\ell^{-4} - 0.0185937\ell^{-2} + 0.989219 - 0.02046875\ell^2 - 0.00109375\ell^4) + (0.00906245\ell^{-2} + 0.00015625 + 0.00109375\ell^2)m^2$$

$$P_{RL6_{1,2}} = (0.000416\ell^{-9} - 0.011291\ell^{-7} - 0.284465\ell^{-5} + 0.319034\ell^{-3} + 0.449396\ell^{-1} - 0.155352\ell - 0.005831\ell^3) m^{-1} + (-0.001249\ell^{-7} + 0.231570\ell^{-5} + 0.694711\ell^{-3} - 0.626405\ell^{-1} + 0.029155\ell + 0.010412\ell^3)m + (0.000833\ell^{-5} - 0.209913\ell^{-3} + 0.020824\ell^{-1} - 0.002082\ell)m^3 - 0.009996\ell^{-1}m^5$$

In $RL6_1$ and $RL6_2$ we observe a demonstration of the dominant unknotting character of the chains and, in $RL6_{1,2}$ the strongly entangled character of the two chain conformation. In order to quantify the extent of complexity of the HOMFLY-PT we propose to employ the spread of the polynomial. This new measure of the complexity of a finite integral Laurent polynomial, such as the HOMFLY-PT,

$$P(\ell, m) = \sum_{i=-k, j=-n}^{i=k, j=n} a_{i,j} \ell^i m^j$$

is defined as follows:

Each point with coordinates (i, j) of the $2k \times 2n$ 2-dimensional integral lattice given the value $|a_{i,j}|$. In analogy with a physical system, we determine the total mass, M , and the "center of mass", (μ_ℓ, μ_m) of this system:

$$M = \sum_{i=-k, j=-n}^{i=k, j=n} |a_{i,j}|$$

$$(\mu_\ell, \mu_m) = \frac{1}{M} \sum_{i=-k, j=-n}^{i=k, j=n} |a_{i,j}|(i, j)$$

We then define the *spread* of $P(\ell, m)$ in analogy with squared radius of gyration of a physical system:

$$sp(P(\ell, m)) = \frac{1}{M} \sum_{i=-k, j=-n}^{i=k, j=n} |a_{i,j}|((i - \mu_\ell)^2 + (j - \mu_m)^2)$$

In the present case the spread of $P_{RL6_{1,2}}(\ell, m)$ is 44.2135 which one may compare with that of the positive Hopf link polynomial having spread 15.7292. Recall that the positive Hopf link has Gauss linking number 1 while RL6 has a comparable Gauss linking number of 1.12954 thereby illustrating the interest in this new measure of entanglement.

4 Random Confined Open Two Component Links

The HOMFLY-PT polynomial of open two component links provides a new method to quantify the extent of entanglement of polymer chains in a melt. This has long been an objective of researchers concerned with the nature of material systems in engineering, chemistry, biology, and physics. Model conformations of polymers of polymers can be obtained using computer simulations. From a historical perspective, one strategy has been to “tighten” the system of open chains, without moving termini, so as to localize physical obstructions at isolated points, called “entanglements”, that are then used to characterize the system [26]. The topology of knots and links in systems composed of closed chains have been used to assess the presence of entanglement using the algebraic topology of the Gauss linking number [17]. The linking number has been extended to systems of oriented open chains using the Gauss linking integral [20]. Scaling characteristics of polymer chains can be obtained by studying random walks. In particular, the behavior of random walks in confined spaces can provide information about similarly confined polymer chains such as biopolymers in a cell. Here, we apply this thinking to pairs of random walks whose initial termini lie within a ball of fixed radius, with a uniform distribution, and are confined to lie in this ball. For example, consider the case of walks with 15, 20, 25, 30, and 40 steps, see Figures 7, 9, 11, 13, and 15, respectively. In Figure 6, we show the growth of the average absolute value of the Gauss linking number of such chains as a function of the length of the chains.

4.1 Discussion of the HOMFLY-PT polynomials of two component link examples

For single open chains, such as these, the classical knot theory has been extended to open arcs whereby one considers the distribution of knot types, the knot spectrum, defined by collection of closures of the arc termini over the two sphere

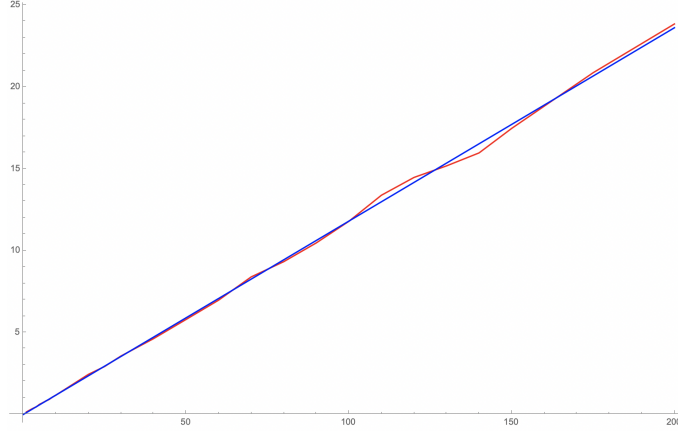


Figure 6: The average absolute value of the Gauss linking number of two random walks confined to a ball of radius 4, as a function of the length of the walks, n . The linear growth is $-0.00834 + 0.118216n$ with $R^2 = 0.9994$, [20].

of directions [14]. As mentioned earlier, Kauffman and Panagioutou [9] describe a theory that defines an average of the Jones polynomial of an open chain over all projection directions. In this paper we propose to associate a HOMFLY-PT polynomial to an open arc by taking the average of the HOMFLY-PT polynomial over all closure directions of an open arc, i.e. the superposition of the knotting spectrum of [14]. Moreover, we propose to associate a HOMFLY-PT polynomial to a pair of oriented open arcs by taking the superposition of the HOMFLY-PT polynomials over all the independent closure directions of the open arcs, thereby taking a superposition of their linking spectrum. This method extends to collections of oriented open chains. Here, we apply this thinking to pairs of random walks whose initial termini lie within a ball of a fixed radius, with a uniform distribution, and are confined to lie within this ball. For example, in the case of a pair of 15 step random walks, Figure 7, the Gauss linking number is 1.0892, and the spectrum is given in Table 7. The average HOMFLY-PT polynomial is

$$(-0.130362\ell^{-5} + 0.583507\ell^{-3} + 0.576426\ell^{-1} - 0.132028\ell + 0.004165\ell^3) m^{-1} + (0.075385\ell^{-5} + 0.284465\ell^{-3} - 0.761000\ell^{-1} + 0.0008330\ell) m + (-0.075385\ell^{-3} - 0.003319\ell^{-1} - 0.000833\ell)m^3$$

whose spread is 28.87. The spectrum of this link is illustrated in Figure 8.

In order to illustrate this new approach to quantifying the growth in entanglement complexity as the length of the chains grows, we first share examples with increasing chain length. In the case of a pair of 20 step random walks,

Figure 9, The Gauss linking number is -0.0456613, and the specturum is given Table 8. The average HOMFLY-PT polynomial is

$$(-0.007189\ell^{-5} + 0.100000\ell^{-3} - 0.633333\ell^{-1} - 0.600000\ell + 0.138562\ell^3) m^{-1} + (0.0071895\ell^{-5} + 0.022222\ell^{-3} - 0.103922\ell^{-1} - 0.137908\ell) m + (-0.0071895\ell^{-3} - 0.0006536\ell^{-1})m^3$$

whose spread is 5.28712. The spectrum of this link is illustrated in Figure 10.

In the case of a pair of 25 step random walks, Figure 11, The Gauss linking number is -1.85846, and the specturum is given Table 9. The average HOMFLY-PT polynomial is

$$(-0.00249895\ell^{-5} + 0.0270721\ell^{-3} - 0.482716\ell^{-1} - 0.2082466\ell + 0.3027905\ell^3) m^{-1} + (0.00083299\ell^{-5} + 0.47938359\ell^{-3} + 0.9204498\ell^{-1} + 0.1724281\ell) m + (-0.000832986\ell^{-3} - 0.4752187\ell^{-1})m^3$$

whose spread is 23.02798. The spectrum of this link is illustrated in Figure 12.

In the case of a pair of 30 step random walks, Figure 13, The Gauss linking number is 0.00715655, and the specturum is given Table 10. The average HOMFLY-PT polynomial is

$$(-0.00249895\ell^{-5} + 0.0270721\ell^{-3} - 0.482716\ell^{-1} - 0.2082466\ell + 0.3027905\ell^3) m^{-1} + (0.00083299\ell^{-5} + 0.47938359\ell^{-3} + 0.9204498\ell^{-1} + 0.1724281\ell) m + (-0.000832986\ell^{-3} - 0.4752187\ell^{-1})m^3$$

whose spread is 3.94706. The spectrum of this link is illustrated in Figure 14.

The estimated HOMFLY-PT polynomial of the link RL6 is:

$$P_{RL6}(\ell, m) = (-0.002082466\ell^{-5} + 0.489796\ell^{-3} + 0.0414493\ell^{-1} - 0.450229\ell - 0.0012495\ell^3 - 0.0012495\ell^5)m^{-1} + (0.002082466\ell^{-5} + 0.006247397\ell^{-3} - 0.4918783\ell^{-1} + 0.00374844\ell^3 + 0.001249479\ell^5)m + (-0.002082466\ell^{-3} - 0.00124948\ell^3)m^3$$

Roughly half of closures of RL6 are negative Hopf links and the other half trivial links, the complexity of the remaining closures expresses a greater degree of linking complexity present in this link.

The spread of $P_{RL6}(\ell, m)$ is 13.8730 while the negative Hopf link polynomial has spread 15.7292. The Gauss linking number of RL6 is -1.12954 compared to -1 for the negative Hopf link.

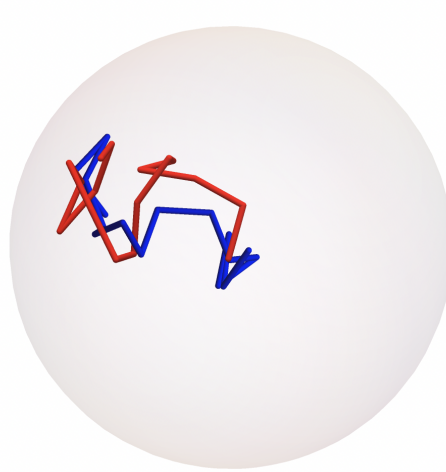


Figure 7: A confined pair of random walks of length 15. The Gauss linking number is 1.0892. The average HOMFLY-PT polynomial is: $(-0.130362\ell^{-5} + 0.583507\ell^{-3} + 0.576426\ell^{-1} - 0.132028\ell + 0.004165\ell^3) m^{-1} + (0.075385\ell^{-5} + 0.284465\ell^{-3} - 0.761000\ell^{-1} + 0.0008330\ell) m + (-0.075385\ell^{-3} - 0.003319\ell^{-1} - 0.000833\ell)m^3$.

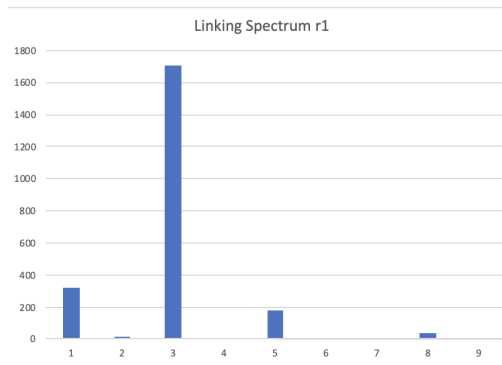


Figure 8: The HOMFLY-PT polynomial spectrum of a confined pair of random walks of length 15.

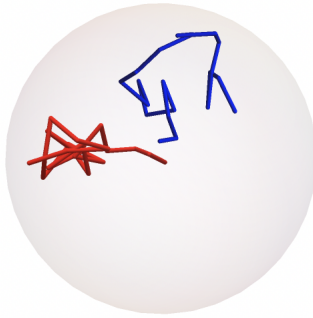


Figure 9: A confined pair of random walks of length 20. The average HOMFLY-PT polynomial is: $(-0.007189\ell^{-5} + 0.100000\ell^{-3} - 0.633333\ell^{-1} - 0.600000\ell + 0.138562\ell^3) m^{-1} + (0.0071895\ell^{-5} + 0.022222\ell^{-3} - 0.103922\ell^{-1} - 0.137908\ell) m + (-0.0071895\ell^{-3} - 0.0006536\ell^{-1})m^3$.

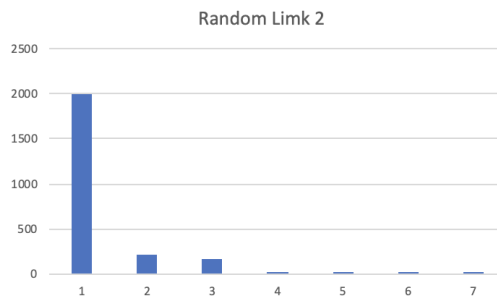


Figure 10: The HOMFLY-PT polynomial spectrum of a confined pair of random walks of length 20.

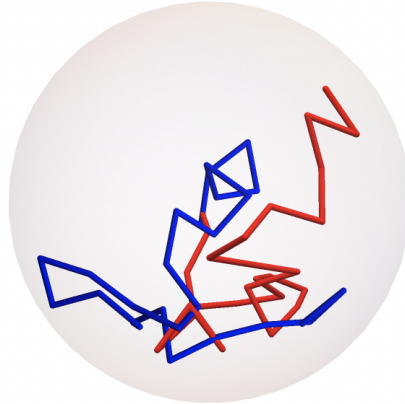


Figure 11: A confined pair of random walks of length 25. The average HOMFLY-PT polynomial is: $(-0.00249895\ell^{-5} + 0.0270721\ell^{-3} - 0.482716\ell^{-1} - 0.2082466\ell + 0.3027905\ell^3) m^{-1} + (0.00083299\ell^{-5} + 0.47938359\ell^{-3} + 0.9204498\ell^{-1} + 0.1724281\ell) m + (-0.000832986\ell^{-3} - 0.4752187\ell^{-1})m^3$.

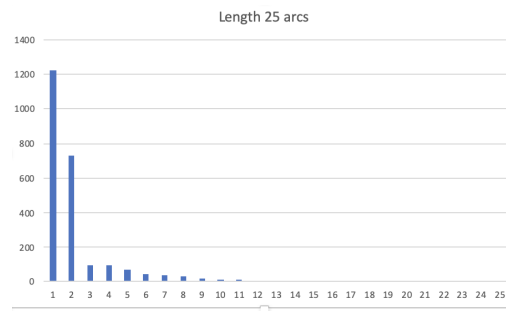


Figure 12: The HOMFLY-PT polynomial spectrum of a confined pair of random walks of length 25.

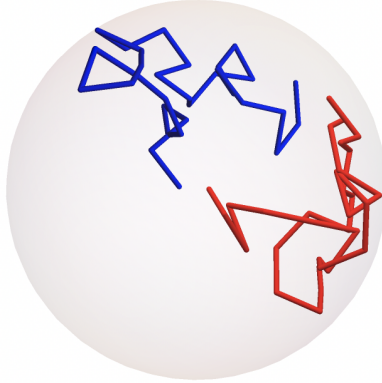


Figure 13: A confined pair of random walks of length 30. The average HOMFLY-PT polynomial is: $(-0.00249895\ell^{-5} + 0.0270721\ell^{-3} - 0.482716\ell^{-1} - 0.2082466\ell + 0.3027905\ell^3) m^{-1} + (0.00083299\ell^{-5} + 0.47938359\ell^{-3} + 0.9204498\ell^{-1} + 0.1724281\ell) m + (-0.000832986\ell^{-3} - 0.4752187\ell^{-1})m^3$.

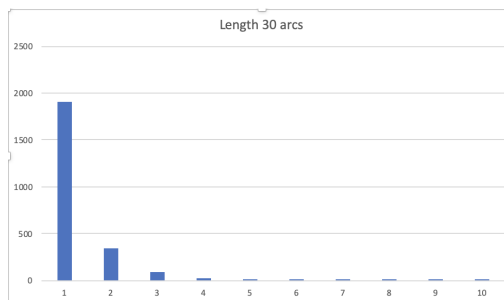


Figure 14: The HOMFLY-PT polynomial spectrum of a confined pair of random walks of length 30.

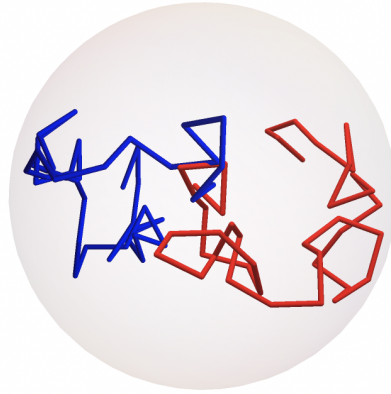


Figure 15: A confined pair of random walks, RL6, of length 40. The average HOMFLY-PT polynomial is $(-0.002082466\ell^{-5} + 0.489796\ell^{-3} + 0.0414493\ell^{-1} - 0.450229\ell - 0.0012495\ell^3 - 0.0012495\ell^5)m^{-1} + (0.002082466\ell^{-5} + 0.006247397\ell^{-3} - 0.4918783\ell^{-1} + 0.00374844\ell^3 + 0.001249479\ell^5)m + (-0.002082466\ell^{-3} - 0.00124948\ell^3)m^3$.

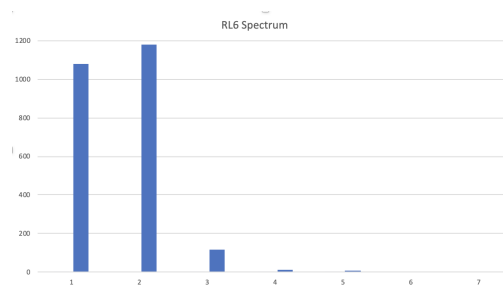


Figure 16: The HOMFLY-PT polynomial spectrum of a confined pair of random walks of length 40, RL6.

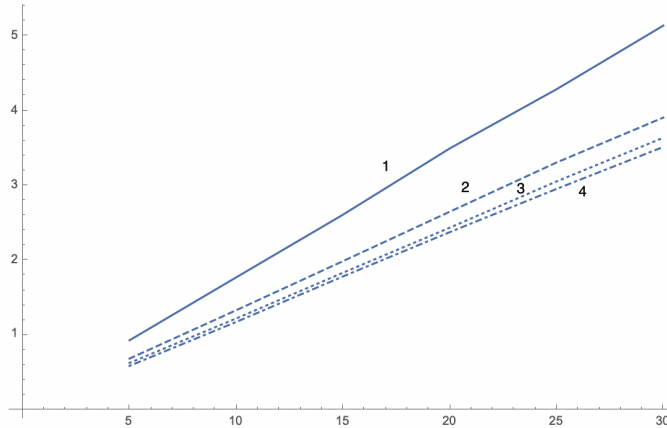


Figure 17: The absolute Gauss linking numbers as a function of length when confined to balls of radius 4 (dot-dashed), 3 (dotted), 2 (dashed) and 1 (solid).

4.2 A study of the HOMFLY-PT polynomials of random open confined two component links

In this section we apply the HOMFLY-PT polynomial to the study of open two component links confined to balls of varying radii. Each edge in each chain is of unit length, the chains have an initial point randomly selected from the confining ball with radii 1, 2, 3, or 4 and have lengths 5, 10, 15, 20, 25, or 30. Each case has a sample size of 10,000.

To set the stage, traditionally one might determine the absolute value of the Gauss linking number for a pair of chains as a measure of their entanglement. The averages of these values as a function of the radius of the ball and the length of the chains of the samples are shown in Figure 17. We observe that the absolute Gauss linking number depends linearly on the length of the chain in a manner depending on the character of confinement, as expected [20]. Considering the absolute Gauss linking number for pairs of chains of link 5, we see that the values decrease monotonically with increasing radius of the confining ball, Figure 18.

While the Gauss linking number provides a traditional measure of link entanglement, the HOMFLY-PT provides a much richer assessment of entanglement for both open and closed two component links due to its capacity for distinguishing topological knot and link types. To quantify the level of entanglement we will first consider two component links of chains with lengths five and ten confined to a ball of radius one. The first question we ask is “How large a sample must one have in order to give a reasonable estimate of the average degree of entanglement of a collection open polygonal chains?”

While it is possible for two equilateral triangles to be Gauss linked, we are interested in more complex entanglement. The closure of a chain of three edges

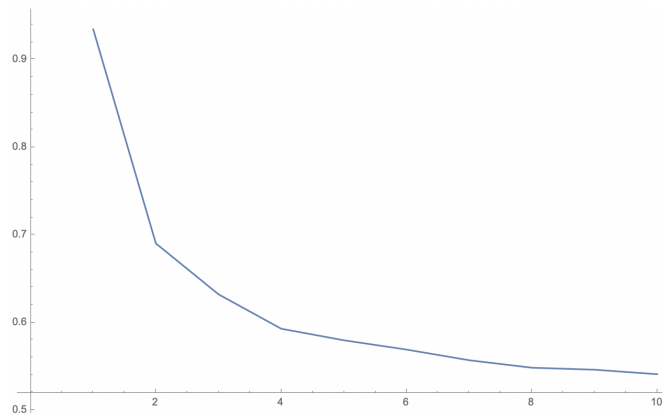


Figure 18: The average absolute Gauss linking numbers of pairs of chains of length 5 confined to balls of radii 1 through 10.

will have five edges, still too few to achieve a trefoil knot as this requires at least six edges. As a consequence, we consider the closure of a chain of five edges which will have a total of seven edges. A chain with seven edges can be one of only of four topological knot types: 0_1 , $\pm 3_1$, and 4_1 . To make a crude estimate of the complexity of the task of assessing the entanglement of collections of open polygonal chains of five edges, one first estimates the number of distinct presentations of closures of five edge polygonal chains. To give an estimate of the complexity of the problem, we can look at the diagrams generated by open curves in 3-space, which can be seen as knotoids (Turaev [29, 1]). For three and four edges, see figure 19, there are very few polygonal knotoids though more than one expects for small numbers of crossings. This changes for five edges, see figure 20 for 37 instances. If one adds the mirror reflections, one estimates rough 74 polygonal knotoids with five edges. The closure to a large 2-sphere adds two additional edges joined to the termini from a point on the 2-sphere. This adds a potential total of 8 crossings of the five edge knotoid for a total of 14 possible crossings and, therefore, 16384 crossing choices. This gives an estimate of a total of 1212416 diagrams, so that 10^5 would be a very cautious estimate of the number of cases.

If one uses this rough estimate of 10^5 presentations, without taking inter crossings into consideration, there are roughly the square this number for the possible cases for two component links. Each edge of one component can over or under cross an edge of the other component once, without taking order into consideration, so one has an additional factor of $16384 = 2^7$ giving a very crude estimate of 1.6×10^{14} different presentations. Using such arguments one can show that the number of distinct link types in each instance is finite and is certainly quite large.

Recall that, for each pair of chains, we consider 2401 closures. We show the

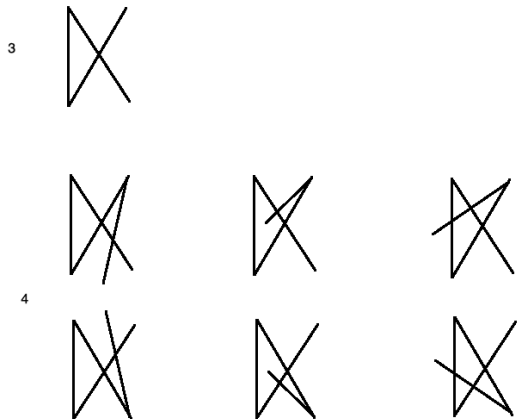


Figure 19: The polygonal knotoids of three and four edge polygons.

growth in the number of distinct HOMFLY-PT polynomials for 10^k samples of size 2401 of two component links of length five for $k = 2, 3, 4$, and 5 in Figure 21. While the number of distinct conformations steadily increases, with an unknown useful upper bound, a consideration of 10,000 sample data for increasing ball radius, Figure 22, suggests that the number of distinct links observed reflects the degree of entanglement as it is largest for the ball of radius one and decreases as the radius increases reflecting the expected decrease in entanglement.

The mean squared radius of gyration for this data suggests a limit of roughly 2.87, Figure 23. Considering the squared radius of gyration for length five links as the ball radius increases, Figure 24, the monotonic increase is consistent with decreasing density and, correspondingly, decreasing entanglement.

With regard to our putative measure of entanglement, the spread of the HOMFLY-PT polynomial, there is visible variation in this range with an average of 5.08, Figure 25. The monotonic decrease in spread with respect to ball radius, Figure 26, reflects the decrease in entanglement with the relaxation of confinement for two component links of length 5.

Consider the case of length 10, for comparison. One observes the growth in the number of distinct HOMFLY-PT polynomials for 10^k samples for $k = 2, 3, 4$, and 5 in Figure 27. Again the number of conformations steadily increases, with an unknown upper bound. The squared radius of gyration suggests a limit of 2.28, Figure 28. With regard to our putative measure of entanglement, the spread of the HOMFLY-PT polynomial, there is visible variation in this range with an average of 15.46, Figure 29.

Although these data suggest that a sample of 100,000 cases or more would be desirable, computational time constraints requires that an analysis of 10,000

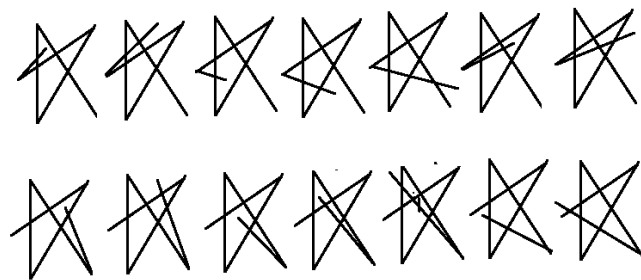
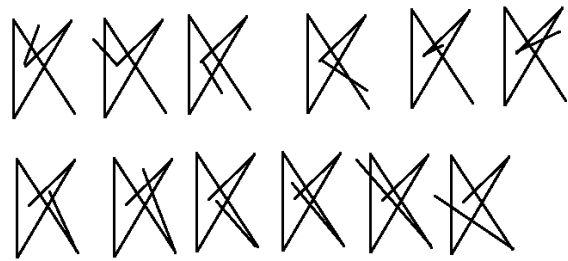
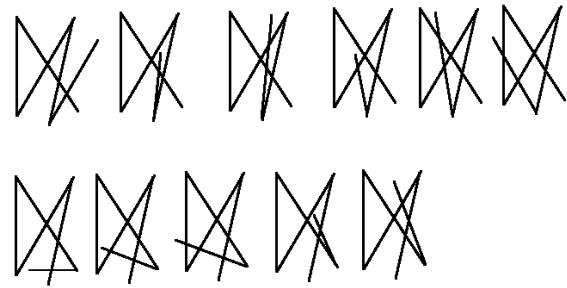


Figure 20: The 37 polygonal knotoids of five edge polygons.

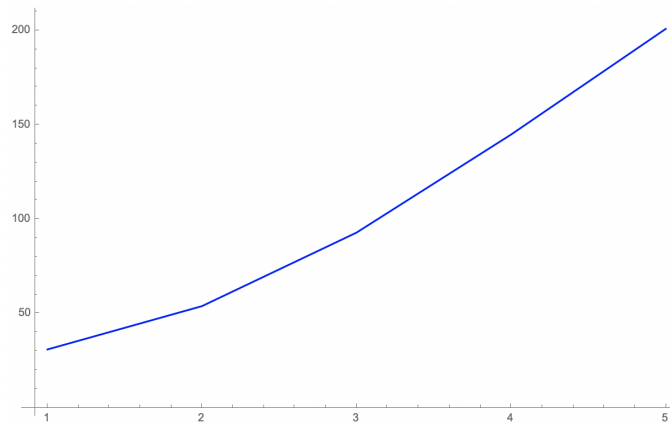


Figure 21: The number of distinct HOMFLY-PT polynomials for length five two component links in a ball of radius 1 for 10^k samples for $k = 2, 3, 4,$ and 5 .

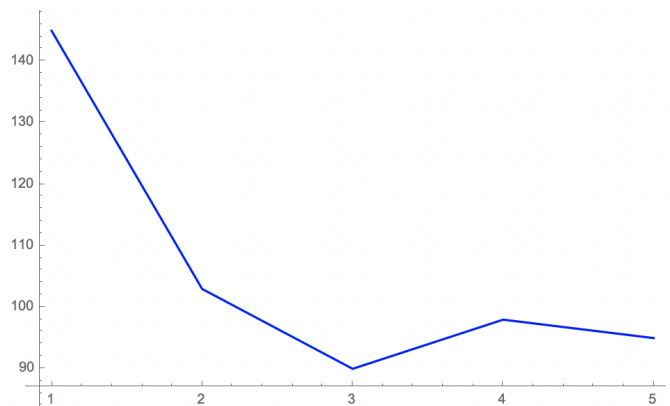


Figure 22: The number of distinct HOMFLY-PT polynomials of length five two component links in a ball of radius k for 10,000 samples with $k = 1, 2, 3, 4,$ and 5

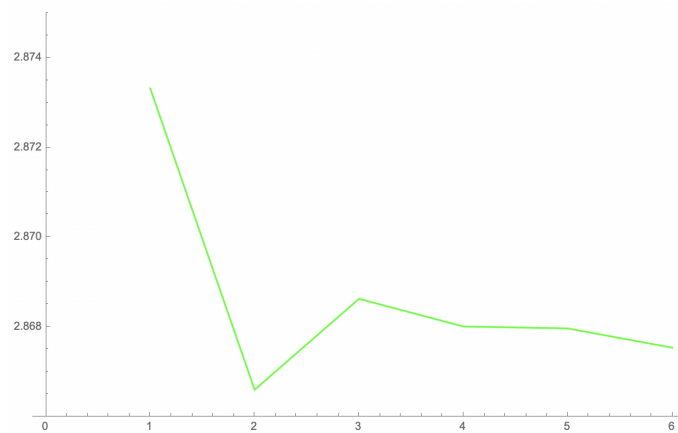


Figure 23: The squared radius of gyration for length five two component links in a ball of radius 1 for 10^k samples for $k = 2, 3, 4, 5$, and 6.

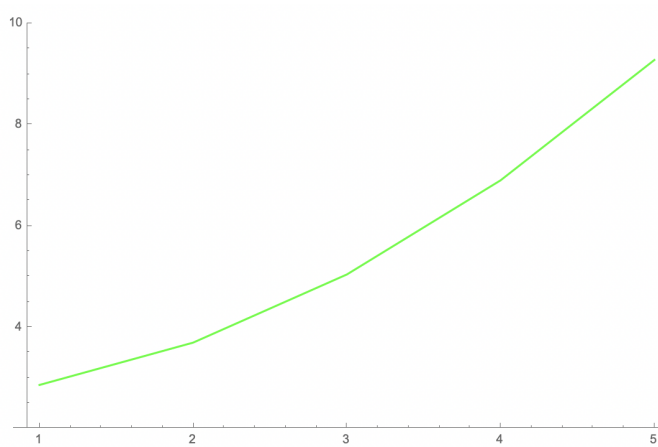


Figure 24: The squared radius of gyration for length five two component links in a ball of radius k for 10,000 samples with $k = 1, 2, 3, 4, 5$, and 6.

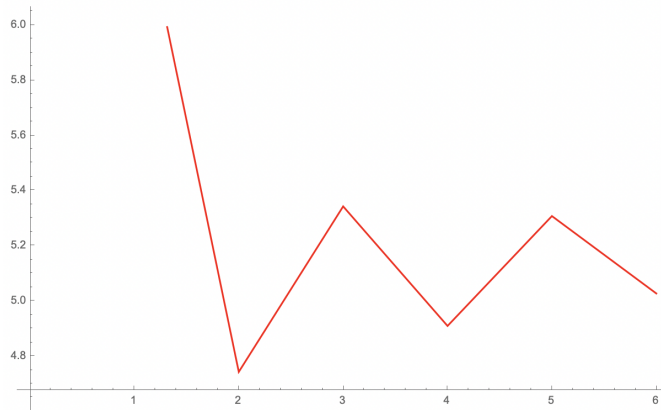


Figure 25: The HOMFLY-PT polynomial spread for length five two component links in a ball of radius 1 for 10^k samples for $k = 2,3,4,5$, and 6.

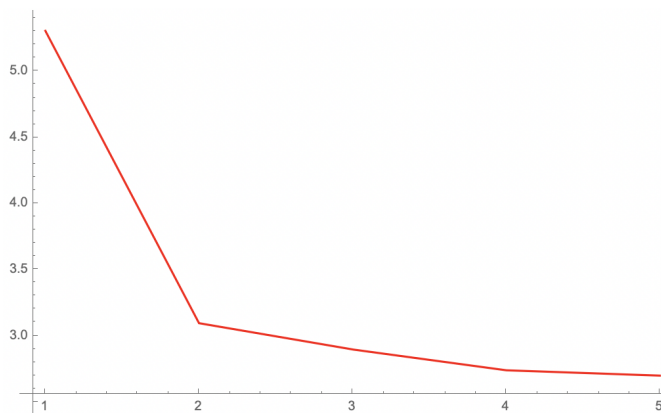


Figure 26: The HOMFLY-PT polynomial spread for length five two component links in a ball of radius k for 10,000 samples with $k = 1,2,3,4$, and 5

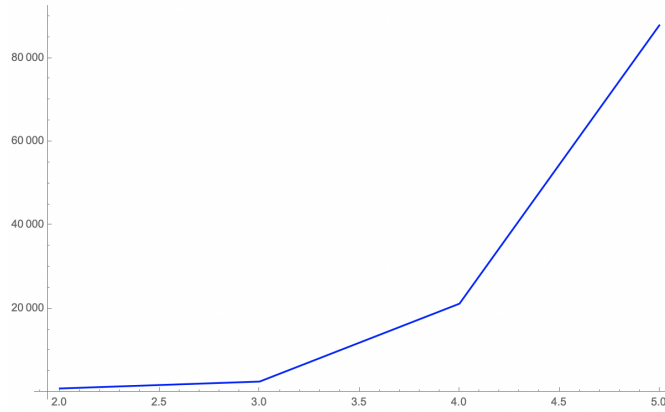


Figure 27: The number of distinct HOMFLY-PT polynomials for length ten two component links in a ball of radius 1 for 10^k samples for $k = 2, 3, 4,$ and 5

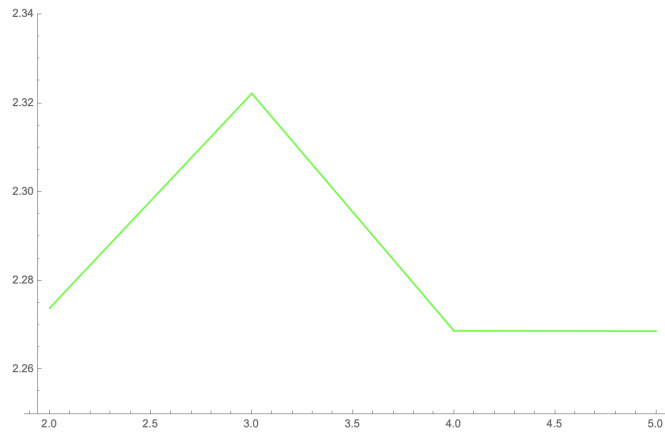


Figure 28: The squared radius of gyration for length ten two component links in a ball of radius 1 for 10^k samples for $k = 2, 3, 4,$ and 5

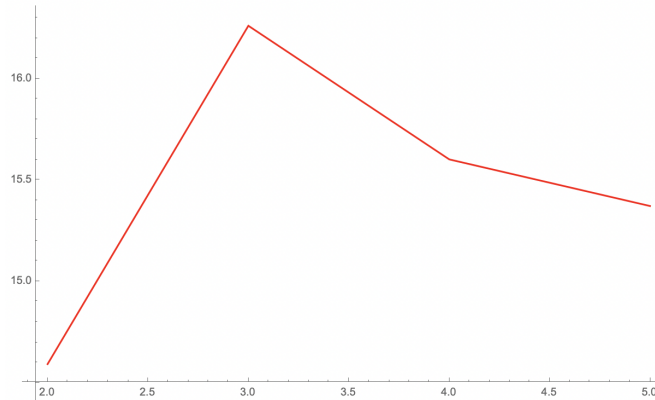


Figure 29: The HOMFLY-PT polynomial spread for length ten two component links in a ball of radius 1 for 10^k samples for $k = 2, 3, 4$, and 5

cases be used to illustrate the effects of confinement and length on our HOMFLY-PT quantification of entanglement.

4.2.1 Consequences of Confinement

To give another perspective on the consequences of confinement we hold the ball radius constant and increase the chain length. In the case of the number of observed distinct HOMFLY-PT polynomials, Figure 30, we are constrained to lengths 5, 10, 15, and 20 due to the computational complexity encountered with increasing length in confinement. The growth of the number quantifies the increasing entanglement as the length of the chains increases. A log analysis shows the number grows as

$$0.00220086\ell^{6.95078}$$

where ℓ is the length of the chain confined to the ball of radius 1. The monotonically decreasing squared radius of gyration with increasing chain length, Figure 31, also reflects the increasing entanglement. Finally, the HOMFLY-PT spread, Figure 32, captures the increasing entanglement.

For the ball of radius 2, one can slightly increase the length of the chains to 25 before computational complexity prevents further increase, Figures 33, 34, and 35. A log analysis shows the number grows as

$$0.00591167\ell^{6.00749}$$

where ℓ is the length of the chain confined to the ball of radius 1. The squared radius of gyration and the HOMFLY-PT show the same behavior as in the case of radius 1.

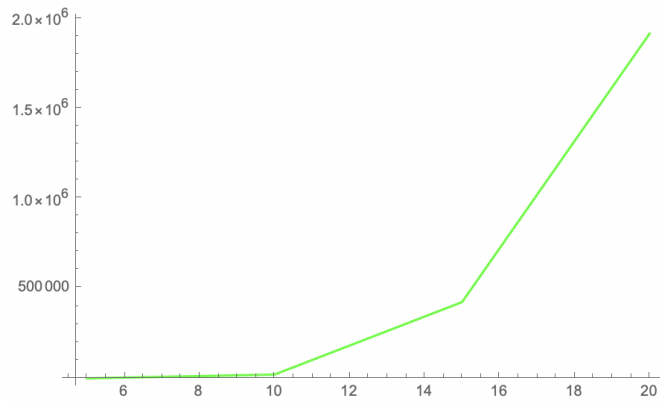


Figure 30: The number of distinct HOMFLY-PT polynomials in a ball of radius 1 for lengths 5, 10, 15, and 20 .

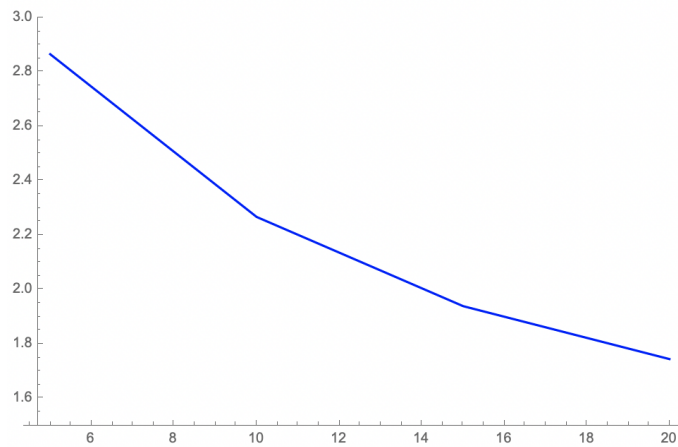


Figure 31: The squared radius of gyration for two component links in a ball of radius 1 for lengths 5, 10, 15, and 20 .

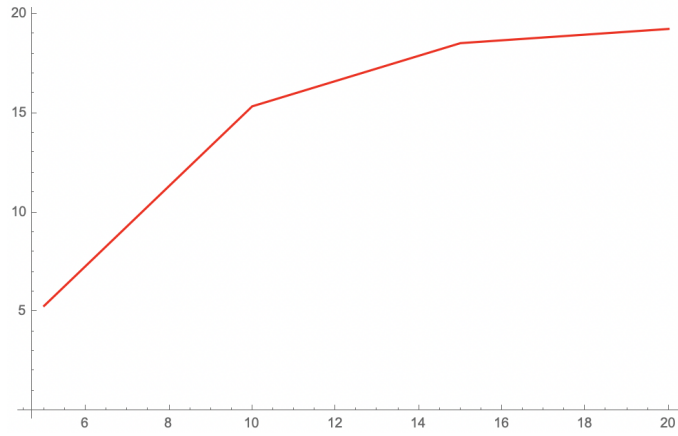


Figure 32: The HOMFLY-PT spread for two component links in a ball of radius 1 for lengths 5, 10, 15, and 20 .

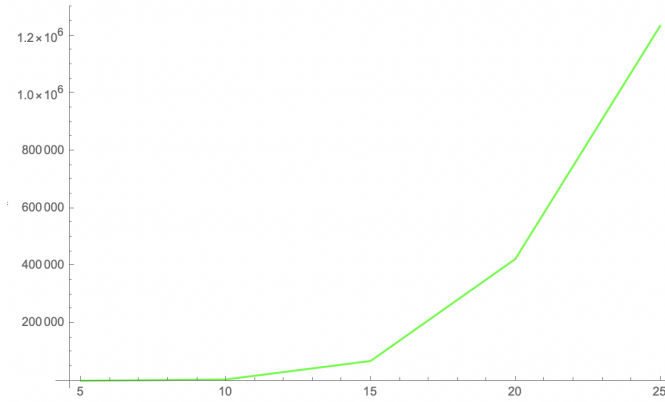


Figure 33: The number of distinct HOMFLY-PT polynomials in a ball of radius 2 for lengths 5, 10, 15, and 20 .

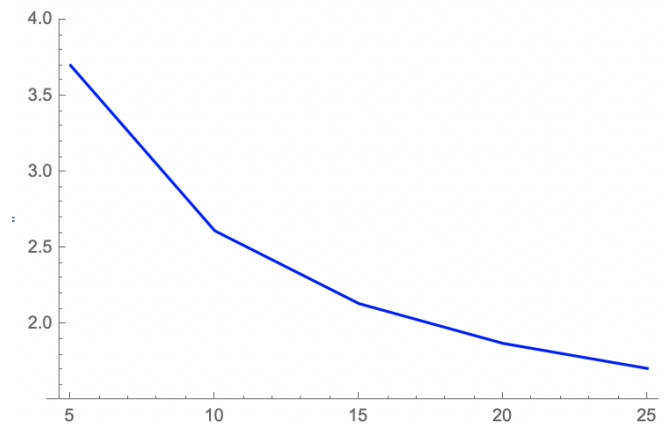


Figure 34: The squared radius of gyration for two component links in a ball of radius 2 for lengths 5, 10, 15, and 20 .

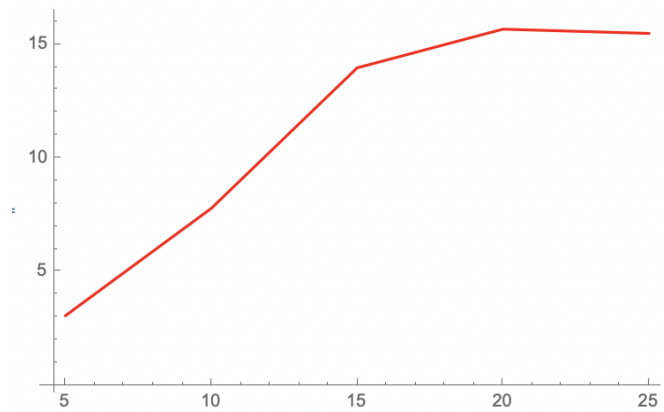


Figure 35: The HOMFLY-PT spread for two component links in a ball of radius 1 for lengths 5, 10, 15, and 20 .

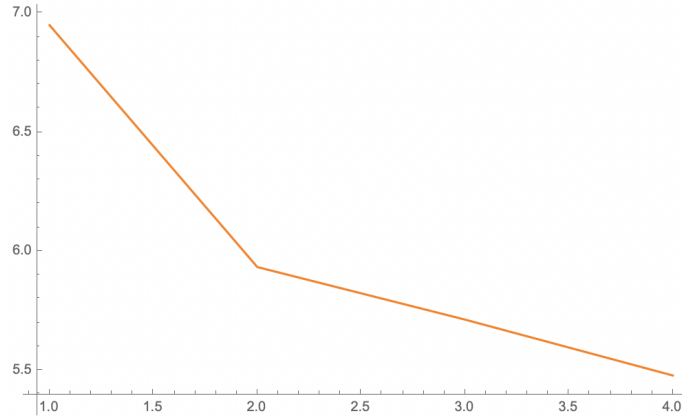


Figure 36: The growth of distinct HOMFLY-PT polynomials is modeled by a power law whose exponent, shown here, decreases with increasing radius of the confining ball reflecting the degree of entanglement as the radius increases.

For a ball of radius 3, the number of distinct HOMFLY-PT polynomials grows as

$$0.00818644\ell^{5.71424}$$

and, for radius 4, the number grows as

$$0.0124913\ell^{5.47958}$$

Figure 36 displays the evolution of the exponent as the radius of the ball increases. For longer links, the degree of entanglement, as reflected in the number of distinct HOMFLY-PT polynomials decreases in a manner similar to that of links of length 5, Figure 37.

The mean squared radius of gyration, Figure 38, confirms the consequences of length versus confinement, with larger values corresponding to, relatively, decreased values of confinement.

The larger values of the spread of the HOMFLY-PT polynomial of the two component link as a function of the ball radius correspond to increased entanglement as a function of chain length and confinement, Figure 39.

5 Discussion

With the objective of employing the HOMFLY-PT to create a quantitative measure of entanglement of two open chains we have defined the average, over independent spatial closures, of the HOMFLY-PT. While it is invariant over orientation preserving Euclidean transformations, i.e. translations and $SO(3)$ rotations, the open Hopf link examples in section 2, is not a diffeomorphism

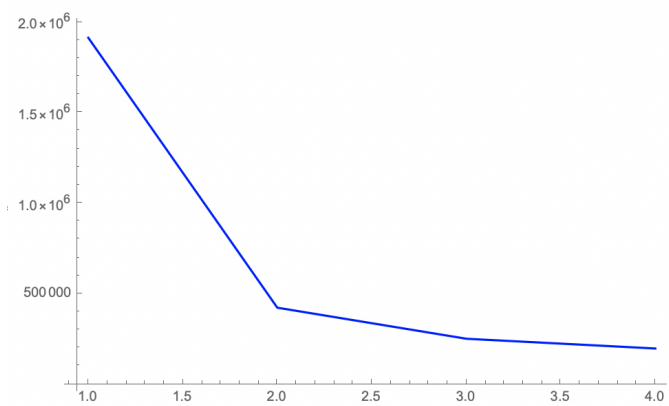


Figure 37: The number of distinct HOMFLY-PT polynomials for chains of length 20 as function of the radius.

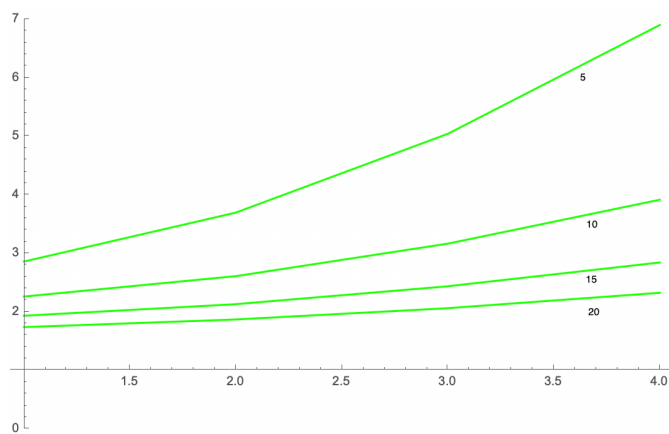


Figure 38: The dependence of squared radius of gyration on the length of the chains and confining ball radius.

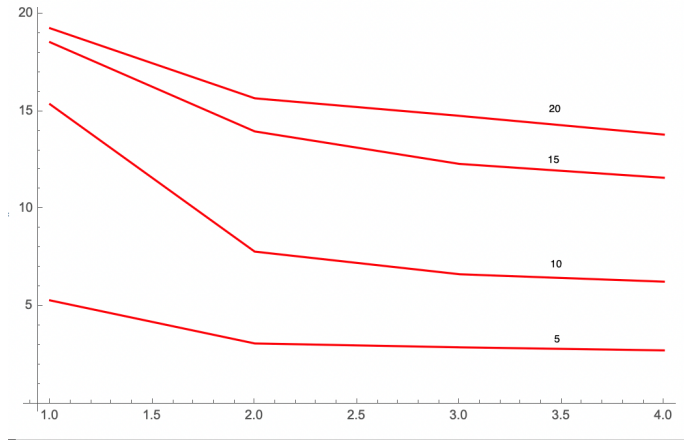


Figure 39: The dependence of the spread of the HOMFLY-PT polynomial of the two component link on the length of the chains and confining ball radius.

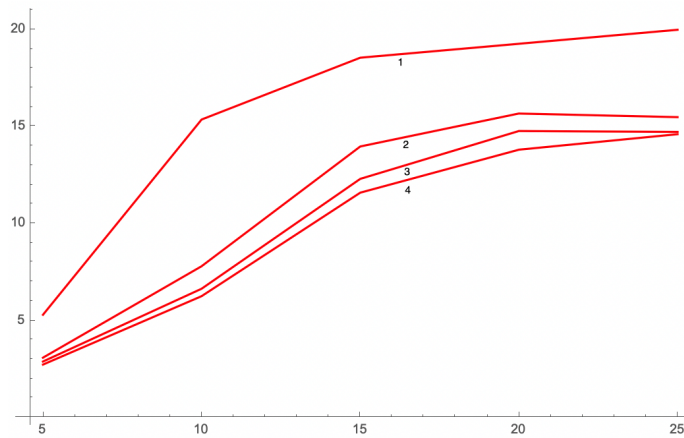


Figure 40: The dependence of the spread of the HOMFLY-PT polynomial of the two component link as a function of the chain length on the length of the chains and confining ball radius.

invariant. In this sense, these examples show that it is similar to the values of the Gauss linking integral [5, 20] but are more geometric than topological in character. Although the Gauss linking number of two oriented closed chains can be found in the HOMFLY-PT polynomial as per proposition 3.1, we have noted that it does not carry over to the average HOMFLY-PT polynomial that we've defined here. Similarly, it seems to have a character distinct from the shape quantities defined by Rogen [24, 23] that are inspired by the Gauss linking integral and related to Vassiliev invariants. Alas, at this point, a useful characterization of the geometric significance of our average HOMFLY-PT has not been identified.

The complexity of the average HOMFLY-PT, even in simple cases such as open Hopf links, leads one to seek a single numerical measure of the quantification. To this end we define the spread of the two variable polynomial in 3.2.3. For one variable polynomials, e.g. the Jones polynomial [8], this would be the radius of gyration of the system of points on the integers with the absolute values of the coefficients placed at the exponents. In this case, the spread would be analogous to the breadth of Jones polynomial and one is provoked to seek an extension of the Kauffman-Murasugi-Thistlethwaite theorem [11, 16, 28] relating the breadth of the Jones polynomial to the number of crossings in a minimal crossing presentation of the link: specifically, the breadth of the Jones polynomial is an upper bound for the number of crossings in a minimal presentation and is achieved only for alternating presentations. At this time there is no known analogue for the HOMFLY-PT polynomial nor is there a version that works for open knots due to the consequences of the averaging procedure..

6 Conclusions

We have suggested the use of the superposition of the HOMFLY-PT polynomials of the spectrum of an open chain [14] to define a HOMFLY-PT of an open chain in 3-space. We have described how the superposition of the HOMFLY-PT polynomials of the random closures of an open two component link can be employed to give a HOMFLY-PT polynomial of the open link whose spread can be understood as a quantifying measure of the degree of entanglement present in the open link. This measure of entanglement is characterized through its estimation for links of length 5 through 30 under confinement to ball of varying radius. While the classic Gauss linking measure of entanglement suggests a linking dependence on the chain length, the spread shows a much more nuanced dependence. The computational complexity of the HOMFLY-PT polynomial is a constraining factor in this study that, therefore, suggests that employing a less sensitive such as the Alexander polynomial or Vassiliev invariants [10] should be studied in the hope that they will, nevertheless, be able to give a useful measure of entanglement using the superposition of closures.

Appendix A: Open Hopf Links

HOMFLY-PT Type	Number of Observations	HOMFLY-PT polynomial
0_1^2	199	$(-\ell^{-1} - \ell)m^{-1}$
2_1^2	2183	$(\ell + \ell^3)m^{-1} - \ell m$
-2_1^2	1	$(\ell^{-3} + \ell)m^{-1} - \ell^{-1}m$
4_1^2	9	$(-\ell^3 - \ell^5)m^{-1} + (-\ell - \ell^3)m$
4_1^2	5	$(-\ell^3 - \ell^5)m^{-1} + (3\ell^3 + \ell^5)m - \ell^3m^3$
5_1^2	4	$(-\ell^{-1} - \ell)m^{-1} + (\ell^{-1} + 2\ell + \ell^3)m - \ell m^3$

Table 2: This data reports the links types observed for the 2401 closures of the open Hopf Link A shown in Figure 3. The link types labelled 4_1^2 are members of a family of four topologically distinct oriented differentiated by orientation and mirror reflection.

HOMFLY-PT Type	Number of Observations	HOMFLY-PT polynomial
0_1^2	1680	$(-\ell^{-1} - \ell)m^{-1}$
2_1^2	420	$(\ell + \ell^3)m^{-1} - \ell m$
-2_1^2	301	$(\ell^{-3} + \ell)m^{-1} - \ell^{-1}m$
4_1^2	0	$(-\ell^3 - \ell^5)m^{-1} + (-\ell - \ell^3)m$
4_1^2	0	$(-\ell^3 - \ell^5)m^{-1} + (3\ell^3 + \ell^5)m - \ell^3m^3$
5_1^2	0	$(-\ell^{-1} - \ell)m^{-1} + (\ell^{-1} + 2\ell + \ell^3)m - \ell m^3$

Table 3: The data reports the links types observed for the 2401 closures for the open Hopf Link B shown in Figure 3

HOMFLY-PT Type	Number of Observations	HOMFLY-PT polynomial
0_1^2	1132	$(-\ell^{-1} - \ell)m^{-1}$
2_1^2	1055	$(\ell + \ell^3)m^{-1} - \ell m$
-2_1^2	189	$(\ell^{-3} + \ell)m^{-1} - \ell^{-1}m$
4_1^2	25	$(-\ell^3 - \ell^5)m^{-1} + (-\ell - \ell^3)m$
4_1^2	0	$(-\ell^3 - \ell^5)m^{-1} + (3\ell^3 + \ell^5)m - \ell^3m^3$
5_1^2	0	$(-\ell^{-1} - \ell)m^{-1} + (\ell^{-1} + 2\ell + \ell^3)m - \ell m^3$

Table 4: The data reports the links types observed for the 2401 closures for the open Hopf Link C shown in Figure 3

HOMFLY-PT Type	Number of Observations	HOMFLY-PT polynomial
0_1^2	668	$(-\ell^{-1} - \ell)m^{-1}$
2_1^2	1637	$(\ell + \ell^3)m^{-1} - \ell m$
-2_1^2	62	$(\ell^{-3} + \ell)m^{-1} - \ell^{-1}m$
4_1^2	34	$(-\ell^3 - \ell^5)m^{-1} + (-\ell - \ell^3)m$
4_1^2	0	$(-\ell^3 - \ell^5)m^{-1} + (3\ell^3 + \ell^5)m - \ell^3 m^3$
5_1^2	0	$(-\ell^{-1} - \ell)m^{-1} + (\ell^{-1} + 2\ell + \ell^3)m - \ell m^3$

Table 5: The data reports the links types observed for the 2401 closures for the open Hopf link shown in Figure 3

HOMFLY-PT Type	Number of Observations	HOMFLY-PT polynomial
0_1^2	238	$(-\ell^{-1} - \ell)m^{-1}$
2_1^2	2131	$(\ell + \ell^3)m^{-1} - \ell m$
-2_1^2	4	$(\ell^{-3} + \ell)m^{-1} - \ell^{-1}m$
4_1^2	27	$(-\ell^3 - \ell^5)m^{-1} + (-\ell - \ell^3)m$
4_1^2	1	$(-\ell^3 - \ell^5)m^{-1} + (3\ell^3 + \ell^5)m - \ell^3 m^3$
5_1^2	0	$(-\ell^{-1} - \ell)m^{-1} + (\ell^{-1} + 2\ell + \ell^3)m - \ell m^3$

Table 6: The data reports the links types observed for the 2401 closures for the open Hopf link shown in Figure 3

B Two component link examples

This appendix contains the data reporting the spectrum of distinct link types observed in the 2401 closures of some examples of open two component links at the length of the chains varies.

References

- [1] Benjamin A. Burton. The Next 350 Million Knots. In Sergio Cabello and Danny Z. Chen, editors, *36th International Symposium on Computational Geometry (SoCG 2020)*, volume 164 of *Leibniz International Proceedings in Informatics (LIPIcs)*, pages 25:1–25:17, Dagstuhl, Germany, 2020. Schloss Dagstuhl–Leibniz-Zentrum für Informatik.
- [2] Millett K. C. and E Panagiotou. Entanglement transitions in one-dimensional confined fluid flow. *Fluid Dynamics Research*, tbd(tbd):tbd, 2016.
- [3] Pierre-Gilles De Gennes. *Scaling concepts in polymer physics*. Cornell University Press, 1979.

HOMFLY-PT Type	Number of Observations	HOMFLY-PT polynomial
0_1^2	320	$(-\ell^{-1} - \ell)m^{-1}$
2_1^2	10	$(\ell + \ell^3)m^{-1} - \ell m$
-2_1^2	1711	$(\ell^{-3} + \ell)m^{-1} - \ell^{-1}m$
4_1^2	129	$(-\ell^3 - \ell^5)m^{-1} + (-\ell - \ell^3)m$
4_1^2	181	$(-\ell^3 - \ell^5)m^{-1} + (3\ell^3 + \ell^5)m - \ell^3m^3$
5_1^2	2	$(-\ell^{-1} - \ell)m^{-1} + (\ell^{-1} + 2\ell + \ell^3)m - \ell m^3$
-5_1^2	5	$(-\ell^{-1} - \ell)m^{-1} + (\ell^{-3} + 2\ell^{-1} + \ell)m - \ell^{-1}m^3$
6_1^2	1	$(\ell^{-7} + \ell^{-5})m^{-1} + (-\ell^{-5} + \ell^{-3} - \ell^{-1})m$
6_2^2	39	$(\ell^{-7} + \ell^{-5})m^{-1} + (-\ell^{-7} - 2\ell^{-5} - 2\ell^{-3})m + (\ell^{-5} - \ell^{-3})m^3$
6_3^2	3	$(-\ell^{-5} - \ell^{-3})m^{-1} + (2\ell^{-3} + \ell^{-1} + \ell)m - \ell^{-1}m^3$

Table 7: The data reports the link types observed for the 2401 closures for the confined random two component link in Figure 7

HOMFLY-PT Type	Number of Observations	HOMFLY-PT polynomial
0_1^2	2000	$(-\ell^{-1} - \ell)m^{-1}$
2_1^2	212	$(\ell + \ell^3)m^{-1} - \ell m$
-2_1^2	161	$(\ell^{-3} + \ell)m^{-1} - \ell^{-1}m$
4_1^2	15	$(-\ell^3 - \ell^5)m^{-1} + (-\ell - \ell^3)m$
4_1^2	1	$(-\ell^3 - \ell^5)m^{-1} + (3\ell^3 + \ell^5)m - \ell^3m^3$
-4_1^2	11	$(-\ell^{-5} - \ell^{-3})m^{-1} + (\ell^{-5} + 3\ell^{-3})m - \ell^{-3}m^3$
5_1^2	0	$(-\ell^{-1} - \ell)m^{-1} + (\ell^{-1} + 2\ell + \ell^3)m - \ell m^3$
-5_1^2	1	$(-\ell^{-1} - \ell)m^{-1} + (\ell^{-3} + 2\ell^{-1} + \ell)m - \ell^{-1}m^3$
6_1^2	0	$(\ell^{-7} + \ell^{-5})m^{-1} + (-\ell^{-5} + \ell^{-3} - \ell^{-1})m$
6_2^2	0	$(\ell^{-7} + \ell^{-5})m^{-1} + (-\ell^{-7} - 2\ell^{-5} - 2\ell^{-3})m + (\ell^{-5} - \ell^{-3})m^3$
6_3^2	0	$(-\ell^{-5} - \ell^{-3})m^{-1} + (2\ell^{-3} + \ell^{-1} + \ell)m - \ell^{-1}m^3$

Table 8: The data reports the link types observed for the 2401 closures for the confined random two component link in Figure 9

- [4] S.F Edwards. The statistical mechanics of polymerized material. *Proc. Phys. Soc.*, 92(1):9–16, 1976.
- [5] Gauss K F. Zur mathematischen theorie der electrodynamischen wirkungen. *Werke vol 5 Konigl. Ges. Wiss. Gottingen*, page 605, 1877.
- [6] P. Freyd, D. Yetter, J. Hoste, W. B. R. Lickorish, K.C. Millett, and A. Ocneanu. A new polynomial invariant of knots and links. *Bull. Amer. Math. Soc. (N.S.)*, 12(2):239–246, 1985.

HOMFLY-PT Type	Number of Observations	HOMFLY-PT polynomial
0_1^2	0	$(-\ell^{-1} - \ell)m^{-1}$
2_1^2	727	$(\ell + \ell^3)m^{-1} - \ell m$
-2_1^2	68	$(\ell^{-3} + \ell)m^{-1} - \ell^{-1}m$
4_1^2	41	$(-\ell^3 - \ell^5)m^{-1} + (-\ell - \ell^3)m$
-4_1^2	4	$(-\ell^{-5} - \ell^{-3})m^{-1} + (-\ell^{-3} - \ell^{-1})m$
4_1^2	6	$(-\ell^3 - \ell^5)m^{-1} + (3\ell^3 + \ell^5)m - \ell^3 m^3$
-4_1^2	2	$(-\ell^{-5} - \ell^{-3})m^{-1} + (\ell^{-5} + 3\ell^{-3})m - \ell^{-3}m$
5_1^2	1227	$(-\ell^{-1} - \ell)m^{-1} + (\ell^{-1} + 2\ell + \ell^3)m - \ell m$
-5_1^2	0	$(-\ell^{-1} - \ell)m^{-1} + (\ell^{-3} + 2\ell^{-1} + \ell)m - \ell^{-1}m$
6_1^2	0	$(\ell^{-7} + \ell^{-5})m^{-1} + (-\ell^{-5} + \ell^{-3} - \ell^{-1})m$
6_2^2	0	$(\ell^{-7} + \ell^{-5})m^{-1} + (-\ell^{-7} - 2\ell^{-5} - 2\ell^{-3})m$
6_3^2	0	$(\ell^{-5} - \ell^{-3})m^3$
-6_3^2	15	$(-\ell^{-5} - \ell^{-3})m^{-1} + (2\ell^{-3} + \ell^{-1} + \ell)m - \ell^{-1}m$
221r3	36	$(/\ell\ell + \ell\ell^3)m^{-1}(-2\ell^{-1} - 5\ell - 2\ell^3)m + (\ell^{-1} + 4\ell +$
222r3	98	
223r3	2	
224r3	5	
225r3	3	
227r3	98	
228r3	14	
230r3	2	
232r3	2	
233r3	1	
234r3	2	
236r3	13	
228r3	1	
239r3	29	
240r3	2	
241r3	2	
242r3	1	

Table 9: The data reports the link types observed for the 2401 closures for the confined random two component link in Figure 11

- [7] S. Igram, K. C. Millett, and E. Panagiotou. Resolving critical degrees of entanglement in olympic ring systems. *J. Knot Theory Ramifications*, 25(14):1650081, 2016.
- [8] V. Jones. Hecke algebra representations of braid groups and link polynomials. *Ann. of Math.*, 126(2):335–388, 1987.
- [9] L. Kauffman and E. Panagiotou. Knot polynomials of open and closed curves. *Proc. R. Soc. A.*, 476(2240):20200124, 20, 2020.

HOMFLY-PT Type	Number of Observations	HOMFLY-PT polynomial
0_1^2	1905	$(-\ell^{-1} - \ell)m^{-1}$
2_1^2	347	$(\ell + \ell^3)m^{-1} - \ell m$
-2_1^2	91	$(\ell^{-3} + \ell)m^{-1} - \ell^{-1}m$
4_1^2	19	$(-\ell^3 - \ell^5)m^{-1} + (-\ell - \ell^3)m$
4_1^2	10	$(-\ell^3 - \ell^5)m^{-1} + (3\ell^3 + \ell^5)m - \ell^3m^3$
-4_1^2	0	$(-\ell^{-5} - \ell^{-3})m^{-1} + (\ell^{-5} + 3\ell^{-3})m - \ell^{-3}m^3$
5_1^2	0	$(-\ell^{-1} - \ell)m^{-1} + (\ell^{-1} + 2\ell + \ell^3)m - \ell m^3$
-5_1^2	0	$(-\ell^{-1} - \ell)m^{-1} + (\ell^{-3} + 2\ell^{-1} + \ell)m - \ell^{-1}m^3$
6_1^2	0	$(\ell^{-7} + \ell^{-5})m^{-1} + (-\ell^{-5} + \ell^{-3} - \ell^{-1})m$
-6_1^2	2	$(\ell^5 + \ell^7)m^{-1} + (-\ell^1 + \ell^3 - \ell^5)m$
6_2^2	0	$(\ell^{-7} + \ell^{-5})m^{-1} + (-\ell^{-7} - 2\ell^{-5} - 2\ell^{-3})m +$ $(\ell^{-5} - \ell^{-3})m^3$
-6_3^2	4	$(-\ell^3 - \ell^5)m^{-1} + (2\ell^3 - \ell^5 - \ell^7)m + (-\ell^3 + \ell^5)m^3$
6_3^2	0	$(-\ell^{-5} - \ell^{-3})m^{-1} + (2\ell^{-3} + \ell^{-1} + \ell)m - \ell^{-1}m^3$
225r4	20	
226r4	2	
227r4	1	

Table 10: 2401 closures: data for a confined two component random link of arc length 30, Figure 13.

HOMFLY-PT Type	Number of Observations	HOMFLY-PT polynomial
0_1^2	1081	$(-\ell^{-1} - \ell)m^{-1}$
2_1^2	118	$(\ell + \ell^3)m^{-1} - \ell m$
-2_1^2	1181	$(\ell^{-3} + \ell)m^{-1} - \ell^{-1}m$
4_1^2	1	$(-\ell^3 - \ell^5)m^{-1} + (-\ell - \ell^3)m$
-4_1^2	12	$(-\ell^{-5} - \ell^{-3})m^{-1} + (-\ell^{-3} - \ell^{-1})m$
4_1^2	3	$(-\ell^3 - \ell^5)m^{-1} + (3\ell^3 + \ell^5)m - \ell^3m^3$
-4_1^2	5	$(-\ell^{-5} - \ell^{-3})m^{-1} + (\ell^{-5} + 3\ell^{-3})m - \ell^{-3}m^3$
5_1^2	0	$(-\ell^{-1} - \ell)m^{-1} + (\ell^{-1} + 2\ell + \ell^3)m - \ell m^3$
-5_1^2	0	$(-\ell^{-1} - \ell)m^{-1} + (\ell^{-3} + 2\ell^{-1} + \ell)m - \ell^{-1}m^3$
6_1^2	0	$(\ell^{-7} + \ell^{-5})m^{-1} + (-\ell^{-5} + \ell^{-3} - \ell^{-1})m$
-6_1^2	0	$(\ell^5 + \ell^7)m^{-1} + (-\ell^1 + \ell^3 - \ell^5)m$
6_2^2	0	$(\ell^{-7} + \ell^{-5})m^{-1} + (-\ell^{-7} - 2\ell^{-5} - 2\ell^{-3})m +$ $(\ell^{-5} - \ell^{-3})m^3$
-6_3^2	0	$(-\ell^3 - \ell^5)m^{-1} + (2\ell^3 - \ell^5 - \ell^7)m + (-\ell^3 + \ell^5)m^3$
6_3^2	0	$(-\ell^{-5} - \ell^{-3})m^{-1} + (2\ell^{-3} + \ell^{-1} + \ell)m - \ell^{-1}m^3$

Table 11: 2401 closures: data for a confined two component random link of arc length 40, Figure 15.

- [10] L. Kauffman and E. Panagiotou. Vassiliev measures of complexity for open and closed curves in 3-space. *Arxiv*, (2104.12275), 2021.
- [11] Louis H. Kauffman. State models and the jones polynomial. *Topology*, 26(3):395–407, 1987.
- [12] W. B. R. Lickorish and K. C. Millett. A polynomial invariant of oriented links. *Topology*, 26(1):107–141, 1987.
- [13] W. B. R. Lickorish and K. C. Millett. The new polynomial invariants of knots and links. *Math Mag*, 61(1):3–23, 1988.
- [14] K. C. Millett, A. Dobay, and A. Stasiak. Linear random knots and their scaling behavior. *Macromolecules*, 38(2):601–606, 2005.
- [15] K. C. Millett and B. M. Sheldon. Tying down open knots: A statistical method of identifying open knots with applications to proteins. In *Physical and numerical models in knot theory*, volume 36 of *Ser. Knots Everything*, pages 203–217. World Sci. Publishing, Singapore, 2005.
- [16] K. Murasugi. On invariants of graphs with applications to knot theory. *Trans. Amer. Math. Soc.*, 314(1):1–49, 1989.
- [17] B. G. Nielsen, P. Røgen, and H. G. Bohr. Gauss-integral based representation of protein structure for predicting the fold class from the sequence. *Math. Comput. Modelling*, 43(3 - 4):401 – 412, 2006.
- [18] W. Niemyska, K. C. Millett, and J. I. Sulkowska. Gln-a method to reveal unique properties of lasso type topology in proteins. *Nature Scientific Reports*, 2020.
- [19] E. Panagiotou. The linking number in systems with periodic boundary conditions. *J. Comput. Phys.*, 300:533 – 573, 2015.
- [20] E. Panagiotou, K. C. Millett, and S. Lambropoulou. The linking number and the writhe of uniform random walks and polygons in confined spaces. *J. Phys. A: Math. Theor.*, 43(4):1 – 28, 2010.
- [21] E. Panagiotou, K. C. Millett, and S. Lambropoulou. Quantifying entanglement for collections of chains in models with periodic boundary conditions. *Procedia IUTAM*, 7:251–260, 2013.
- [22] E. Panagiotou, K. C. Millett, S. Lambropoulou, C. Tzoumanekas, and D. N. Theodorou. A study of the entanglement in systems with periodic boundary conditions. *Prog. of Theo. Physics Sup.*, 191:10, 2011.
- [23] P. Røgen and H. Bohr. A new family of global shape descriptors. *Math. Biosci.*, 182(2):167–187, 2003.

- [24] P. Røgen and B. Fain. Automatic classification of protein structure by using gauss integrals. *Proceeding of the National Academy of Sciences*, 100(1):119–124, 2006.
- [25] E. J. Rawdon, K. C. Millett, J. I. Sulkowska, and A. Stasiak. Knot localization in proteins. *Biochem. Soc. Trans.*, 41(2):538–541, 2013.
- [26] B. Rubenstein and E. J. Helfand. Statistics of the entanglement of polymers: concentration effects. *J. Chem Phys*, 82(2477):2477 – 2483, 1985.
- [27] J. I. Sulkowska, E. J. Rawdon, K. C. Millett, J. N. Onuchic, and A. Stasiak. Conservation of complex knotting and slipknotting patterns in proteins. *Proc. Natl. Acad. Sci. USA*, 109(26):E1715–E1723, 2012.
- [28] Morwen B. Thistlethwaite. An upper bound for the breadth of the jones polynomial. *Mathematical Proceedings of the Cambridge Philosophical Society*, 193(3):451–456, 1988.
- [29] V. Turaev. Knotoids. *Osaka J. Math.*, (49):195 – 223, 2012.